

Predictive Switching Control Technique for Three Phase B4 Inverter Using FLC for Torque Control of an Induction Motor Drive

K. Roopa Reddy

Assistant Professor, ANURAG Group of Institutions, India.

Akhila .V

M.Tech, ANURAG Group of Institutions, India.

Abstract – The induction motor drive set with B4 inverter was proposed for reducing the inverter cost, however, the instability in the current due to the fluctuations of dc link voltage is the major drawback. Keeping the factors in view, the torque and stator flux were controlled in a predictive way. Balancing the currents is achieved forcefully by stator flux control method which leads to better results. The effects of the voltage offset due to the two dc-link capacitors are also modeled and controlled in a best possible way using predictive control. To enhance the results of the cost function instead of PI controller, the fuzzy logic controller has been used which helped in giving a good dynamic performance by creating good torque reference values. The simulations of proposed techniques were carried out in the MATLAB/Simulink environment. The torques, as well as stator flux ripples, were comparatively less in the fuzzy logic controller using predictive model.

Index Terms – Cost function, four-switch inverter, induction motor drives, model predictive control, fuzzy logic controller.

1. INTRODUCTION

This variable speed drives using the traditional three-phase inverters and squirrel cage induction machines have already found the widespread in practical applications, for example, Pumps, Industrial Drives, Fans and Blowers. To achieve the cost optimization component minimization option could exist for both that of the machine and the converter, the detailed study of the best optimization is proposed by Vander Broeck and Van Wyk [1] which helped in choosing a different simplified system. Although this kind of cost reduction is the outlay of the output performance. The concept of B4 inverter played an impact to solve the open/short circuit fault conditions of the B6 inverter which indeed attracted many researchers [2]-[10]. Although B4 inverter attracted many researchers the below-listed disadvantages compared with normal B-6 inverters are yet to be compressed.

- 1.Reduction of dc-link voltage ripple.
- 2.Current unbalances due to the capacitor center tap voltage.
- 3.Torque and flux control of the device.

Compensation scheme in order to mitigate the effects of the current distortions for four switch inverter has been proposed by J.Kim, K.Nam and J.Hong [12] as its performance is being limited in the low-frequency region, the voltage errors are derived and compensation method is proposed to diminish the outcome of dc-link voltage ripples, a paper was proposed by J.K.Pedersen, D.O. Neacsu and F.Blaabjerg [11] and a control method for the compensation of unbalanced voltage supply which helps in eliminating the pulsating current in the bus of a voltage source is investigated and analyzed.

The works mentioned earlier helped in improving the B4 inverter performance, however not keeping the drive system flux and torque into account. With the development of fast and powerful processors, and attention has been drawn to use the Model Predictive Control (MPC) in power electronics [19].

In this paper, predictive torque control is used and various constraints and nonlinearities are included all the concerned factors and taken into consideration and apart from that the dynamic performances improvement is also been considered as a challenge by using the fuzzy logic controller to get effective cost function output which eventually helps in selecting the best voltage vector and the sampling interval is also decreased by giving good and fast results and effectively emulating the B6 inverter.

2. MODEL PREDICTIVE CONTROL

A different kind of control approach for the drive system is predictive control approach. In this approach, a system is considered and it is modeled to obtain a cost function wherein various nonlinearities and constraints could be included into it to obtain the best selection in a predictive point of view.

Model predictive control has the ability to make the number of selections condensed out of the many finite selections, thus making an advantageous approach for a power converter and even speeds up the process output.

The working of a model predictive control is done such that the

control action is obtained in a way that the system variables are brought very close to the desired reference causing a negligible error [13]. In real time the control, prediction, and measurement at the same instant cannot be obtained, hence a two-step ahead prediction is usually carried out thus giving fast and dynamic outputs.

A. Comparison Between Classical Controllers And MPC

To underline the differences of the MPC approach with traditional linear control methods, a comparison table is given in below Table I. Traditional linear controllers with modulation are restricted due to their classic feedback structure.

Moreover, the bandwidth and exact working of the controller will depend on how dominant the nonlinearities are. MPC uses a full prediction of the system, and the feedback is also included in the cost function. This control method is easy and requires no modulation techniques for the control of different power electronic converters and various kinds of variables or internal control loops. The drive signals for the power switches

are generated directly by the controller.

FCS-MPC is practically very simple and powerful since it considers the discrete nature of power converters and microprocessors. However, the approach can be applied without significant changes to any type of power converter or induction drive system.

3. MODELING OF THE B4 INVERTER AND IM

A. Intrinsic Voltage Vector of a B4 Inverter

Unlike the B6 topology, The B4 topology consists of a two-leg inverter. In this model, the 4 switches are considered as (T₁-T₄). The second leg apart from the first leg which has two capacitors in it is having the switching states as (T₁-T₂) and the third leg switching states are (T₃-T₄), for easy conventions these switches can be denoted as binary variables S_A and S_B, wherein binary “0” is considered closed state of lower switch and “1” as the closed state of the upper switch as shown in the Fig.1.

Table. I

Difference between traditional controller and MPC

DESCRIPTION	TRADITIONAL CONTROLLER	MPC
Control block diagram		
Modulation	SVM OR PWM	No Modulation
Realization	Analog or digital(after controller discretization)	Direct digital implementation
Switching frequency	Fixed	Controllable
Multivariable	Coupled	Decoupled
Flexibility	Parameter inclusion is not straight and easy	Parameters can be included directly into cost function

Assuming the three-phase voltages to be balanced, the phase-to-neutral voltages V_{AN}, V_{BN}, V_{CN} are given as follows

$$\begin{aligned}
 V_{AO} &= V_{dc2} \\
 V_{BO} &= S_B * (V_{dc1} + V_{dc2}) \\
 V_{CO} &= S_C * (V_{dc1} + V_{dc2})
 \end{aligned}
 \tag{1}$$

From balanced condition, we obtained the value of neutral voltage

$$\begin{aligned}
 V_{AN} + V_{BN} + V_{CN} &= 0 \\
 V_{AO} - V_{NO} + V_{BO} - V_{NO} + V_{CO} - V_{NO} &= 0
 \end{aligned}$$

$$V_{AO} + V_{BO} + V_{CO} - 3 * V_{NO} = 0 \tag{2}$$

$$V_{NO} = (V_{AO} + V_{BO} + V_{CO}) * \frac{1}{3}$$

Now phase voltages are obtained using the above relations

$$\begin{aligned}
 V_{AN} &= -V_{BN} - V_{CN} \\
 &= 2 * V_{NO} - V_{BO} - V_{CO} \\
 &= \frac{2}{3} * (V_{AO} + V_{BO} + V_{CO}) - V_{BO} - V_{CO}
 \end{aligned}
 \tag{3}$$

$$V_{AN} = \frac{2}{3} * (V_{AO}) - \frac{1}{3} * (V_{BO} + V_{CO}) \quad (4)$$

Similarly,

$$V_{BN} = \frac{2}{3} * (V_{BO}) - \frac{1}{3} * (V_{AO} + V_{CO}) \quad (5)$$

$$V_{CN} = \frac{2}{3} * (V_{CO}) - \frac{1}{3} * (V_{AO} + V_{BO}) \quad (6)$$

To obtain three phase voltages in response to the switching states we substitute the above equations

$$V_{AN} = \frac{2}{3} * (V_{AO}) - \frac{1}{3} * (V_{BO} + V_{CO})$$

$$= \frac{2}{3} * (V_{dc2}) - \frac{1}{3} * (S_B V_{dc1} + S_B V_{dc2} + S_C V_{dc1} + S_C V_{dc2})$$

$$V_{AN} = \frac{V_{dc1}}{3} * (-S_B - S_C) + \frac{V_{dc2}}{3} * (2 - S_B - S_C) \quad (7)$$

Similarly the remaining phase voltages with respect to switching states are obtained

$$V_{BN} = \frac{V_{dc1}}{3} * (2 - S_B - S_C) + \frac{V_{dc2}}{3} * (2 - S_B - S_C - 1) \quad (8)$$

$$V_{CN} = \frac{V_{dc1}}{3} * (2 - S_C - S_B) + \frac{V_{dc2}}{3} * (2 - S_C - S_B - 1) \quad (9)$$

where V_{dc1} and V_{dc2} are the upper and the lower dc-link capacitor voltages, respectively.

TABLE II.

B4 INVERTER SWITCH ON AND OUTPUT PHASE VOLTAGES

States		Switch ON		Output phase voltages		
S_B	S_C			V_{AN}	V_{BN}	V_{CN}
0	0	T2	T4	$\frac{2 V_{dc2}}{3}$	$\frac{-V_{dc2}}{3}$	$\frac{-V_{dc2}}{3}$
0	1	T2	T3	$\frac{V_{dc2} - V_{dc1}}{3}$	$\frac{-(2V_{dc2} + V_{dc1})}{3}$	$\frac{(V_{dc2} + 2V_{dc1})}{3}$
1	0	T1	T4	$\frac{V_{dc2} - V_{dc1}}{3}$	$\frac{(V_{dc2} + 2V_{dc1})}{3}$	$\frac{-(2V_{dc2} + V_{dc1})}{3}$
1	1	T1	T3	$\frac{-2 V_{dc1}}{3}$	$\frac{V_{dc1}}{3}$	$\frac{V_{dc1}}{3}$

Considering all the possible combinations of (S_B, S_C) , phase-to-neutral voltages values are given in Table II.

The Clarke transform is applied to the stator voltages that are obtained in the above analysis, in order to obtain the vector

form for easily approachable calculation i.e in terms of $V_{\alpha s}$ and $V_{\beta s}$, where the $V_{\alpha s}$ and $V_{\beta s}$ are the α and β axis stator voltage, respectively.

$$\begin{bmatrix} V_{\alpha s} \\ V_{\beta s} \end{bmatrix} = \frac{2}{3} \begin{bmatrix} 1 & -\frac{1}{2} & -\frac{1}{2} \\ 0 & \frac{\sqrt{3}}{2} & -\frac{\sqrt{3}}{2} \end{bmatrix} \begin{bmatrix} V_{AN} \\ V_{BN} \\ V_{CN} \end{bmatrix} \quad (10)$$

The voltage vectors are expressed by $\vec{v}_s = V_{\alpha} + j * V_{\beta}$. Therefore; the four active voltage vectors (V_1 to V_4) in the $\alpha\beta$ plane are given in Table III.

It is clearly revealed that in Table III, the B4 inverter can only produce four basic non-zero voltage vectors. The basic voltage vectors alter in amplitude and angle in case of dc-link voltage are not equal

TABLE III
VOLTAGE VECTORS OF THE B4 INVERTER

Switching state (S_B, S_C)	Voltage Vectors \vec{v}_s	Vector symbol
00	$\frac{2 \cdot V_{dc2}}{3}$	V_1
10	$\frac{(V_{dc2} - V_{dc1}) - j \cdot \sqrt{3}(V_{dc1} + V_{dc2})}{3}$	V_2
11	$\frac{(V_{dc2} - V_{dc1}) + j \cdot \sqrt{3}(V_{dc1} + V_{dc2})}{3}$	V_3
01	$\frac{-2 \cdot V_{dc1}}{3}$	V_4

It is clearly revealed in the Table III, the B4 inverter can only produce four basic non-zero voltage vectors. The basic voltage vectors alter in amplitude and angle in case of dc-link voltage are not equal

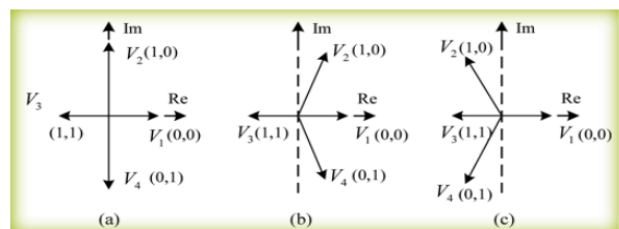


Fig. 1. Voltage vectors of the B4 inverter in the case of: (a) $V_{dc1} = V_{dc2}$, (b) $V_{dc1} < V_{dc2}$, and (c) $V_{dc1} > V_{dc2}$.

The values of the upper and lower capacitance for a constant value of $V_{dc} / 2$ and the four voltage vectors produced by the four kinds of switching combination are represented in Fig. 1(a)

Ripple in that of the two capacitor voltages will cause deviation of the four vectors from its previous positions when the $V_{dc} / 2$

value is constant without ripples. The vector positions are presented in Fig. 1(b) and (c) for two different cases as in $V_{dc1} < V_{dc2}$ and $V_{dc1} > V_{dc2}$, respectively. Therefore, the vector positions are calculated as given in Fig. 3.

for predicting its future values

B. Machine Equations

Stator variables, voltage \vec{v}_s , current \vec{i}_s , and flux $\vec{\Psi}$ are electrically related in a machine according to the given below equation

$$\vec{v}_s = R_s \vec{i}_s + \frac{d\vec{\Psi}_s}{dt} \tag{11}$$

Where R_s denotes stator resistance.

Rotor equation in a given stator frame of reference represents the relation between rotor current \vec{i}_r and rotor flux $\vec{\Psi}_r$ as follows

$$0 = R_r \vec{i}_r + \frac{d\vec{\Psi}_r}{dt} - j\omega \vec{\Psi}_r \tag{12}$$

where R_r represents rotor resistance and ω gives the rotor speed. Stator and rotor flux linkage equations which relate stator and rotor currents are given in (13) and (14), where L_m , L_r , and L_s are the mutual, rotor, and stator inductances, respectively

$$\vec{\Psi}_s = L_s \cdot \vec{i}_s + L_m \cdot \vec{i}_r \tag{13}$$

$$\vec{\Psi}_r = L_m \cdot \vec{i}_s + L_r \cdot \vec{i}_r \tag{14}$$

Electromagnetic torque T_e is expressed in terms of stator current and flux

$$T_e = \frac{3}{2} p \vec{\Psi}_s \times \vec{i}_s \tag{15}$$

where p denotes pole pair in a specific machine.

4. PROPOSED STRATEGY FOR THE B4 INVERTER-FED IM DRIVE

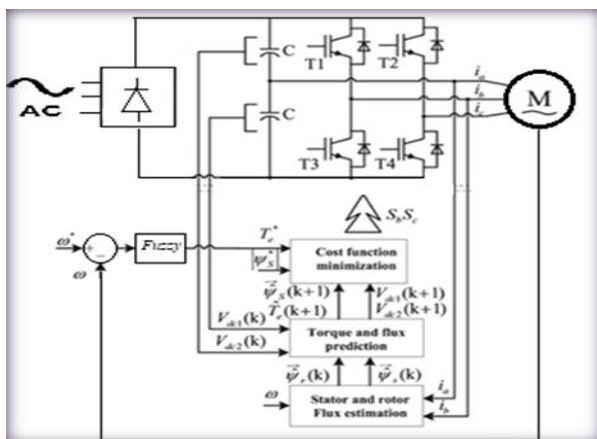


Fig. 2. Structure of the B4 inverter-fed IM drive with fuzzy controller based on the PTC scheme

In the proposed strategy, the basic functioning and the relationship of the control loops is explained as follows, the inner loop control is used for obtaining stator flux and electromagnetic torque for predicting its future values, while in the outer speed loop a fuzzy logic controller is used to obtain reference torque. In any standard PTC scheme to accomplish the required task, a three-step algorithm is carried out: flux estimation flux and torque prediction, and cost function optimization [15],[16].The structural scheme of a B4 inverter-feeding an IM drive-based on PTC is shown in Fig.4

A. Estimation of flux

In B4 based inverter, the voltage ripples lead to different voltage vectors in both amplitude and angular error, considering these points usually in modeling of b4 inverter a current-model-based flux estimation using the instant current and speed signals is adopted instead of voltage-model-based flux estimator as in b6 inverter [20]

$$\vec{\Psi}_r + \tau_r \cdot \frac{d\vec{\Psi}_r}{dt} = -j\tau_r \cdot (\omega_k - \omega) \cdot \vec{\Psi}_r + L_m \cdot \vec{i}_s \tag{17}$$

where $\tau_r = L_r/R_r$, ω_k is the angular speed of a rotating coordinate frame, and ω corresponds to the rotor speed.

Writing (17) in terms of a rotating frame of reference lined up with the stator winding ($\omega_k = 0$) is given as follows:

$$\vec{\Psi}_r + \tau_r \cdot \frac{d\vec{\Psi}_r}{dt} = L_m \cdot \vec{i}_s + j\omega \cdot \tau_r \cdot \vec{\Psi}_r \tag{18}$$

Estimation of stator flux for, the rotor linkage (14) is used to obtain the rotor current in terms of stator currents and estimate the rotor flux. Then, by replacing \vec{i}_r in (13), the stator flux containing terms of \vec{i}_s is obtained .

$$\vec{\Psi}_r = L_m \cdot \vec{i}_s + L_r \cdot \vec{i}_r$$

$$\frac{\vec{\Psi}_r - L_m \cdot \vec{i}_s}{L_r} = \vec{i}_r \tag{19}$$

$$\vec{\Psi}_s = L_s \cdot \vec{i}_s + L_m \cdot \vec{i}_r$$

$$\vec{\Psi}_s = L_s \cdot \vec{i}_s + L_m \cdot \frac{\vec{\Psi}_r - L_m \cdot \vec{i}_s}{L_r} \tag{20}$$

Using Euler-based discretization in (18) and (20), the discrete equations of the rotor and stator flux estimation are as follows

$$\vec{\Psi}_r(k) = \frac{\tau_r}{T_s(1-j\omega\tau_r)} \cdot \vec{\Psi}_r(k-1) + \frac{L_m}{1-j\omega\tau_r} \cdot \vec{i}_s(k) \tag{21}$$

$$\vec{\Psi}_s(k) = K_r \cdot \vec{\Psi}_r(k) + \sigma L_s \cdot \vec{i}_s(k) \tag{22}$$

where T_s corresponds to the sampling time, $K_r = L_m/L_r$ is the rotor coupling factor and $\sigma = 1 - (\frac{L_m^2}{L_s L_r})$ is the total leakage factor.

As it is clear to see in (21), from the rotor flux estimation that is

obtained using the Euler-based discretization there exists only stator currents, without using the command voltages.

B. Prediction of Stator Flux and Electromagnetic Torque

For PTC mechanism the control variables of the proposed strategy such as electromagnetic torque and stator flux are to be predicted at sampling step of k+1.

The stator flux prediction $\vec{\psi}_s(k+1)$ can be obtained by the stator voltage equation. Using the Euler based formula to discretize (11) and for shifting the results to a single time step, the stator flux prediction can be obtained.

Using the Euler based formula to discretize (11) and shifting the result to a single step k+1, the stator flux prediction can be obtained

$$\vec{v}_s = R_s \vec{i}_s + \frac{d\vec{\psi}_s}{dt}$$

Using Euler based discretize formula given below we can obtain the stator prediction as follows.

$$y(t_0 + h) = y(t_0) + hy'(t_0)$$

$$y'(t_0) = \frac{d\vec{\psi}_s}{dt} = \vec{v}_s - R_s \vec{i}_s$$

$$\vec{\psi}_{s(k+1)} = \vec{\psi}_{s(k)} + T_s(\vec{v}_{s(k)} - R_s \vec{i}_{s(k)})$$

$$\vec{\psi}_{s(k+1)} = \vec{\psi}_{s(k)} + T_s \cdot \vec{v}_{s(k)} - R_s T_s \cdot \vec{i}_{s(k)} \quad (23)$$

where T_s is the sampling time used in the PTC algorithm.

The electromagnetic torque prediction can be calculated as

$$\hat{T}_{e(k+1)} = \frac{3}{2} p \cdot \text{Im}\{\vec{\psi}_{s(k+1)} \cdot \vec{i}_{s(k+1)}\} \quad (24)$$

The prediction expression of the stator current $\vec{i}_{s(k+1)}$ is obtained using the equivalent equation of the stator dynamics of an induction machine

$$\vec{v}_s = R_\sigma \cdot \vec{i}_s + L_\sigma \cdot \frac{d\vec{\psi}_s}{dt} - K_r \cdot \left(\frac{1}{\tau_r} - j \cdot \omega\right) \cdot \vec{\psi}_r \quad (25)$$

Where $R_\sigma = R_s + K_r^2 R_r$ corresponds to the equivalent resistance and $L_\sigma = \sigma L_s$ is the leakage inductance of the machine. The last term in (25) represents the cross coupling between the rotor and the stator winding through the induced voltage. Thus, replacing the derivatives with the Euler formula in (25) prediction equation of the stator current \vec{i}_s at the instant k + 1 is obtained

$$\vec{i}_{s(k+1)} = \left(1 + \frac{T_s}{T_\sigma}\right) \cdot \vec{i}_{s(k)} + \frac{T_s}{\tau_\sigma + T_s} \cdot \vec{v}_{s(k)}$$

$$\left\{ \frac{1}{R_p} \cdot \left(\left(\frac{K_r}{\tau_r} - j \cdot k_r \cdot \omega \right) \cdot \vec{\psi}_r + \vec{v}_{s(k)} \right) \right\} \quad (26)$$

Once the predictions of the stator flux (23) and the stator current (26) are obtained, the prediction of the electromagnetic torque can be calculated in (24).

C. Analysis of Fuzzy Logic Controller in the Given Scheme

The conventional PI controllers cannot compensate properly and are too slow due to the sluggish response, finding gain constants are very difficult. Therefore the fuzzy logic controller is being implemented in the feedback path to produce torque reference values.

Fuzzy controller unit consists of four major blocks as shown in the fig.3.

1. Fuzzification interface.
2. Fuzzy rule base.
3. Fuzzy inference engine.
4. Defuzzification

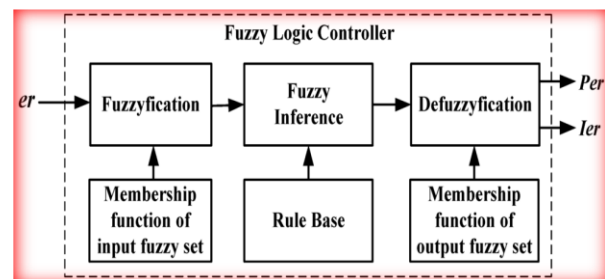


Fig.3.Fuzzy logic controller

Fuzzification interface: The process involves with finding out the input variables in order to perform a scale mapping, in the PTC control error and change in error of speed are considered as the two inputs.

Fuzzy rule base: In this part, certain rules are assigned to get the desired output and accordingly for error in speed the range of parameter limit is set between (-6 to 6) and for change in error the parameter limit is from (0 to 1), type of membership function used is trimf.

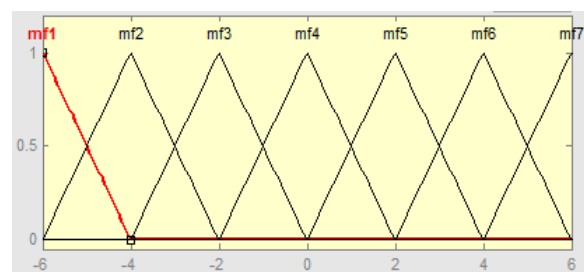


Fig .4. input error as membership functions

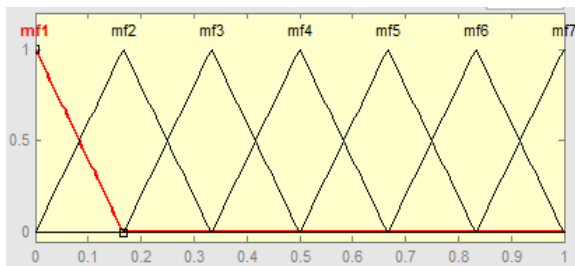


Fig .5. Change as error membership functions

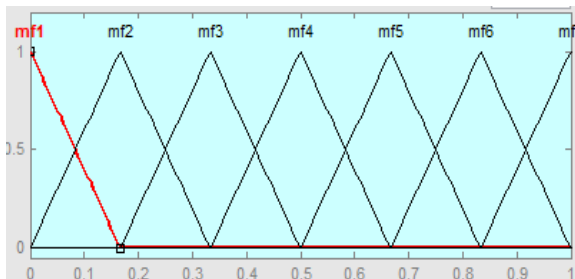


Fig.6. output variable Membership functions

Inference engine: This stage mainly consists of passing the fuzzified inputs through various rules and several compositions

Methods such as “and method min”,” or method max” have been proposed in this literature

Defuzzification: After identifying the outputs from the fuzzy controller the type of method used in this paper is centroid defuzzification and the final output is given to cost function which helps in proper voltage selection and thus improving the dynamic performance.

D. Cost Function Optimization

The important step in predictive control is the optimization of an appropriate control law which is termed as a cost function. As we know that there is one step delay in digital implantation (i.e.) the voltage vector selected at the instant of time k will be applied at k+1 [16]-[19].The delay if not considered can deteriorate the performance. A simple way to compensate this delay is by taking into account calculation time and applies the switching state obtained after the next instant of sampling.

The cost function considering the delay is defined as follows:

$$g_i = \frac{|T_e^* - \hat{T}_e(k+2)_i|}{T_{enom}} + \lambda_0 \frac{||\vec{\Psi}_s^*|| - ||\vec{\Psi}_s(k+2)_i||}{||\vec{\Psi}_s||_{nom}}$$

$$i \in \{1, 2, 3, 4\}$$

$$(30)$$

where *i* denotes the index of the stator voltage vector used to calculate the predictions $\hat{T}_e(k + 2)_i$ and $\vec{\Psi}_s(k + 2)_i$, respectively. The rated torque T_{enom} and the rated stator flux magnitude $||\vec{\Psi}_s||_{nom}$ are used to normalize the cost function

terms. The implementation of all the above said steps put together is shown in form of a flowchart in below Fig.10.

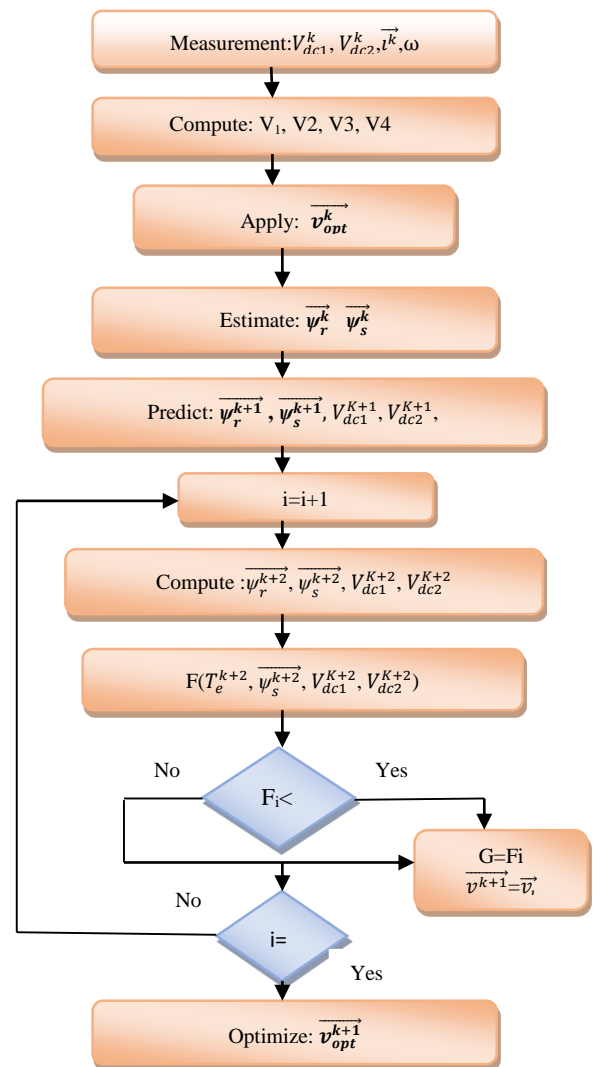


Fig.7. Implementation flowchart of the proposed scheme

E. Voltage Offset Suppression of DC-Link

The initial phase angle of phase “a” current in the two capacitors is inappropriate which causes voltage deviations [14] as shown in Fig.3. Therefore suppressing the voltage offset is necessary for better performance.

In order to compensate for the offset, we consider one of the switching states i.e. $V_4 (1, 0)$ as shown in fig.11. Using Kirchoff's law for the current loops i_{dc1} and i_{dc2} are obtained. A similar procedure can be followed for the other three vectors.

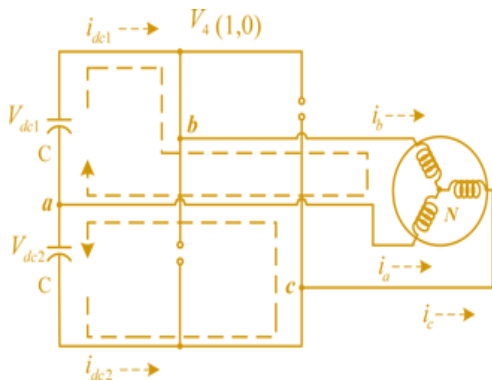


Fig. 8. Current paths in the switching state V4

DC-Link current as a function of switching states is as follows:

$$i_{dc1} = i_b \cdot S_B + i_c \cdot S_C \tag{32}$$

$$i_{dc2} = i_b \cdot (1 - S_B) + i_c \cdot (1 - S_C) \tag{33}$$

where i_{dc1} and i_{dc2} are the upper and the lower dc-link currents and i_b and i_c are the phase currents. With the above-obtained currents (32),(33), the capacitor voltages are formulated

$$\hat{V}_{dc1} = V_{dc1} + \frac{1}{C} \int_{t_0}^t (-i_{dc1})dt$$

$$\hat{V}_{dc2} = V_{dc2} + \frac{1}{C} \int_{t_0}^t (-i_{dc2})dt \tag{34}$$

where C is the dc-link capacitance.

To discretize (32),(33) and (34) we choose Euler based formula and shift the obtained result to a single time step and applied at time “k” for currents and at time “k+1” for voltages $V_{dc1}(k+1)$ and $V_{dc2}(k+1)$ and are obtained as shown.

$$i_{dc1}(k) = i_b(k) \cdot S_B + i_c(k) \cdot S_C$$

$$i_{dc2}(k) = i_b(k) \cdot (1 - S_B) + i_c(k) \cdot (1 - S_C) \tag{35}$$

$$\hat{V}_{dc1}(k + 1) = V_{dc1}(k) - \frac{1}{C} i_{dc1}(k) \cdot T_s$$

$$\hat{V}_{dc2}(k + 1) = V_{dc2}(k) + \frac{1}{C} i_{dc2}(k) \cdot T_s \tag{36}$$

Considering the time delay and including voltage offset suppression a new cost function is obtained by adding the third term to (31).

$$g_i = \frac{|T_e^* - \hat{T}_e(k+2)_i|}{T_{enom}} + \lambda_0 \frac{\left| \left| \hat{\Psi}_s^* \right| - \left| \hat{\Psi}_s(k+2)_i \right| \right|}{\left| \hat{\Psi}_s \right|_{nom}}$$

$$+ \lambda_{dc} \frac{|\hat{V}_{dc1}(k+2)_i - \hat{V}_{dc2}(k+2)_i|}{V_{dc}}, \quad i \in \{1, 2, 3, 4\} \tag{37}$$

where V_{dc} is dc-link voltage, which can be obtained by $V_{dc} = V_{dc1} + V_{dc2}$, λ_{dc} is the weighting factor of the dc-link capacitor voltage offset suppression.

5. ANALYSIS AND DISCUSSION ON WEIGHTING FACTORS

In the proposed scheme, it is clear from (37) that the parameters to be adjusted are the weighting factors. As there is no proper method to obtain the optimum values of these parameters, these values are obtained by a simulation-based process. The ratings and parameters of the induction machine and B-4 inverter used in the simulation are listed in Table IV.

TABLE IV
B4 MOTOR AND INVERTER PARAMETERS

Parameters	Values
DC-link voltage	540V
DC-link upper capacitor(C ₁)	2040μF
DC-link upper capacitor (C ₂)	2040μF
Dead time	4μs
Induction motor	
Rated power	2.2KW
Rated voltage	380V
Rated speed	1430 r/min
Rated current	4.9 A
Rated frequency	50Hz
Number of poles	4
Stator resistance (R _s)	2.804Ω
Stator leakage inductance (L _s)	10.33mH
Rotor resistance(R _r)	2.178 Ω
Rotor leakage inductance (L _r)	10.33mH
Magnetizing inductance (L _m)	319.7mH
Nominal flux-linkage	0.6Wb
Rated torque	14N-m

A. Stator Flux Weighting Factor λ_0

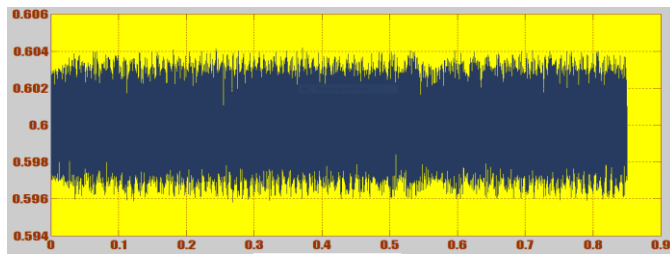
λ_0 is assigned as a weighting factor which proportionally values the importance of the torque versus flux control, $\lambda_0=1$ indicates both are given same preference. However, to obtain the balanced currents a higher weighting factor λ_0 is expected (e.g, $\lambda_0=3$).

The simulation results for various time intervals using the proposed scheme during a speed reversal maneuver from 500 to -500 r/min at 50% rated load torque for cases of $\lambda_0=3$ and $\lambda_0=1$ are shown in Fig.12 and Fig.13 and a comparable study is drawn from it, wherein a higher ripple factor is observed when compared to the previous case. Hence tuning factor λ_0 will be kept at a value of ($\lambda_0=3$).

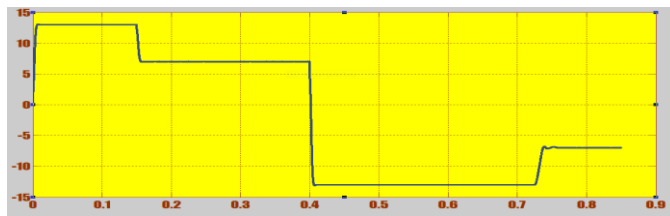


Time (s)

(a)



Time (s)
(b)

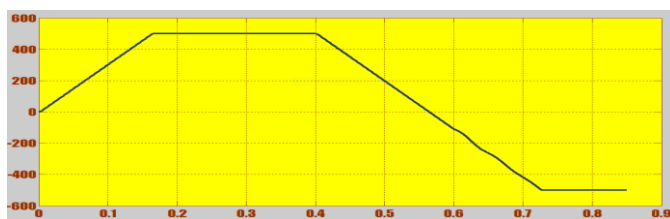


Time (s)
(c)

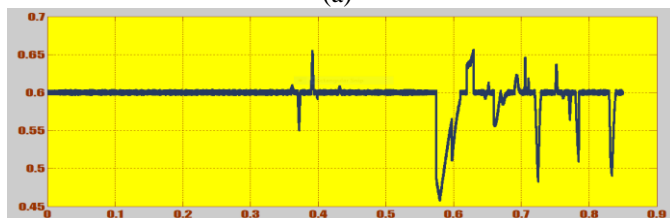


Time (s)
(d)

Fig. 9. Simulated waveforms during a speed-reversal maneuver at 50% rated load torque at $\lambda_0 = 3$ for (1) Speed, (2) stator flux, (3) developed torque, and (4) stator current behaviors using the proposed scheme in a B4 inverter fed IM



(a)



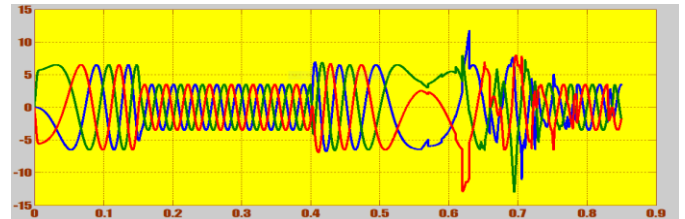
Time (s)
(b)

(b)



Time (s)

(c)



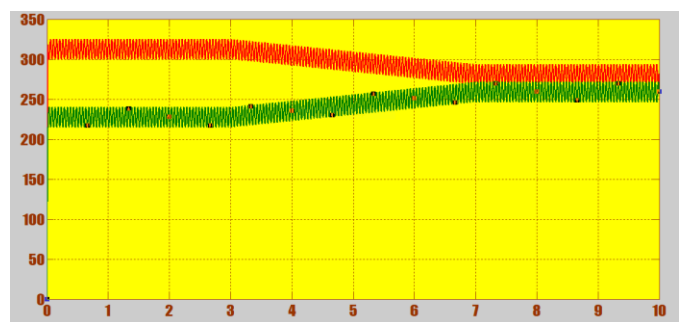
Time (s)

(d)

Fig.10. Simulated waveforms during a speed-reversal maneuver at 50% rated load torque at $\lambda_0 = 1$ for . (1) Speed, (2) stator flux, (3) developed torque, and (4) stator current behaviors using the proposed scheme in a B4 inverter fed IM

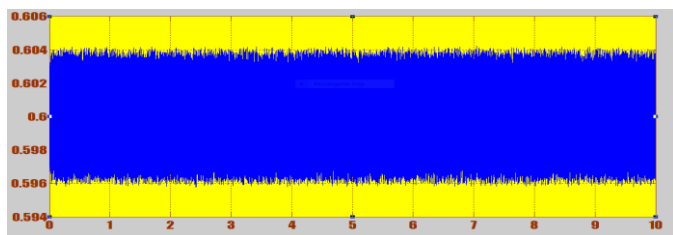
B. Capacitor Voltages Offset Suppression Weighting Factor λ_{dc}
 The assignment of λ_{dc} as weighting factor is to increase or decrease its relative importance of the DC-Link capacitor voltage offset suppression versus the control performance. The simulation results for different cases of λ_{dc} are shown in Fig.14 and 15 at the speed of 500 r/min with a torque of 10 N · m for (1) $\lambda_{dc}=1000$ and (2) $\lambda_{dc}=2000$.

We can notice the effect of voltage until 3sec at that instant the offset term is added and we can see the capacitor voltage converges. The converging time both cases are approximately 1sec but a significant stator flux and torque ripples are exhibited in steady state. In consideration of good performance obtained weighting factor will be kept at a value of $\lambda_{dc}=1000$



Time (s)

(a)



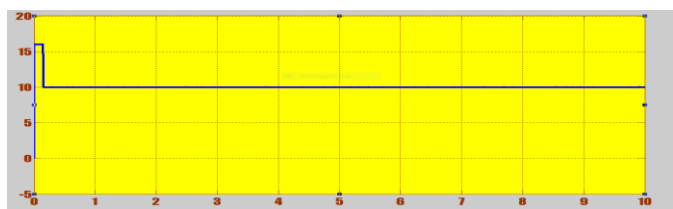
Time (s)

(b)



Time (s)

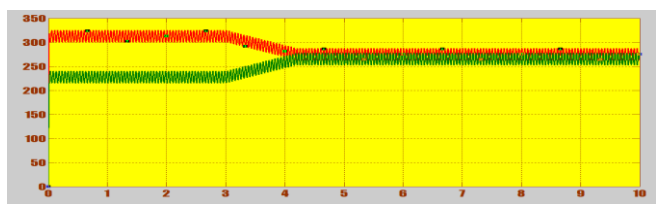
(c)



Time (s)

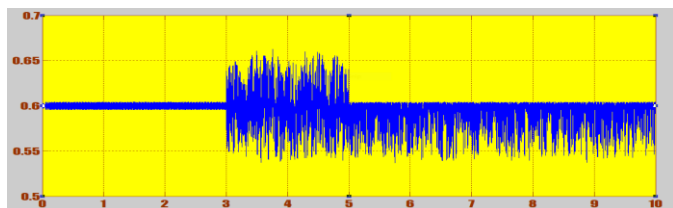
(d)

Fig. 11. Simulated (1) Capacitor voltages, (2) stator flux, (3) speed, and (4) developed torque behaviors during a voltage suppression method applied ($\lambda_{dc} = 2000$).



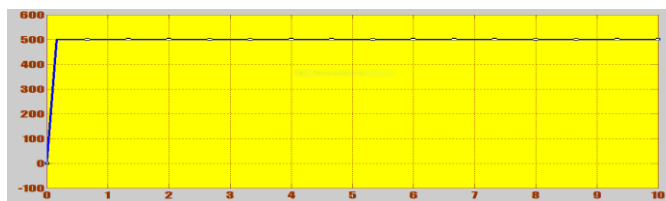
Time (s)

(a)



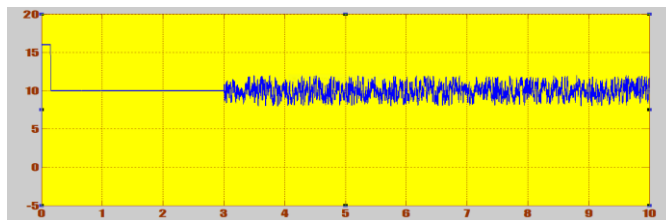
Time (s)

(b)



Time (s)

(c)



Time (s)

(d)

Fig. 12. Simulated. (1) Capacitor voltages, (2) stator flux (3) speed, and (4) developed torque behaviors during a voltage suppression method applied ($\lambda_{dc} = 1000$).

6. CONCLUSION

In this paper, a B4 inverter fed IM drive is implemented in detail. The paper is segregated into various sections and analysis of each component and parameters are studied. In order to obtain the required voltage vector selection, we have analyzed the intrinsic voltages vectors of a B4 inverter in order to apply the outputs from S_B and S_C to the switches, flux estimation is done and the next stage is stator flux and electromagnetic torque prediction. Using the predictive and reference values cost function is designed. The importance of weighting factors as also considered in detail along with the voltage offset suppression in the DC-Link. The above implementation helps in cost reduction and is found acceptable for high performance industrial variable-speed-drive applications. The usage of the fuzzy controller has been advantageous in reducing the ripple content of stator flux ripples. The results show the robustness of the proposed technique in comparison with PI control technique.

REFERENCES

- [1] H. W. Van der Broeck and J. D. Van Wyk, "A comparative investigation of a three-phase induction machine drive with a component minimized voltage-fed inverter under different control options," *IEEE Trans. Ind. Appl.*, vol. IA-20, no. 2, pp. 309–320, Mar. 1984.
- [2] B. A. Welchko, T. A. Lipo, T. M. Jahns, and S. E. Schulz, "Fault tolerant three-phase AC motor drive topologies: A comparison of features, cost, and limitations," *IEEE Trans. Power Electron.*, vol. 19, no. 4, pp. 1108–1116, Jul. 2004.
- [3] R. L. D. Ribeiro, C. B. Jacobina, E. R. C. da Silva, and A. M. N. Lima, "Fault-tolerant voltage-fed PWM inverter AC motor drive systems," *IEEE Trans. Ind. Electron.*, vol. 51, no. 2, pp. 439–446, Apr. 2004.

- [4] D. Campos-Delgado, D. Espinoza-Trejo, and E. Palacios, "Fault-tolerant control in variable speed drives: A survey," *Electric Power Appl., IET*, vol. 2, no. 2, pp. 121–134, 2008.
- [5] F. Jen-Ren and T. A. Lipo, "A strategy to isolate the switching device fault of a current regulated motor drive," in *Proc. IEEE Ind. Appl. Soc. Annu. Meeting, Conf. Rec.*, 1993, vol. 2, pp. 1015–1020.
- [6] T. Elch-Heb and J. P. Hautier, "Remedial strategy for inverter-induction machine system faults using two-phase operation," in *Proc. 5th Eur. Conf. Power Electron. Appl.*, 1993, vol. 5, pp. 151–156.
- [7] P. N. Enjeti and A. Rahman, "A new single-phase to three-phase converter with active input current shaping for low cost AC motor drives," *IEEE Trans. Ind. Appl.*, vol. 29, no. 4, pp. 806–813, Jul./Aug. 1993.
- [8] A. M. S. Mendes, X. M. Lopez-Fernandez, and A. J. M. Cardoso, "Thermal performance of a three-phase induction motor under fault tolerant operating strategies," *IEEE Trans. Power Electron.*, vol. 23, no. 3, pp. 1537–1544, May 2008.
- [9] D. Sun, Z. Y. He, Y. K. He, and Y. F. Guan, "Four-switch inverter fed PMSM DTC with SVM approach for fault tolerant operation," in *Proc. IEEE Int. Electric Machines Drives Conf.*, 2007, vol. 1–2, pp. 295–299.
- [10] L. Tian-Hua, F. Jen-Ren, and T. A. Lipo, "A strategy for improving reliability of field-oriented controlled induction motor drives," *IEEE Trans. Ind. Appl.*, vol. 29, no. 5, pp. 910–918, Sep./Oct. 1993.
- [11] F. Blaabjerg, D. O. Neacsu, and J. K. Pedersen, "Adaptive SVM to compensate DC-Link voltage ripple for four-switch three-phase voltage-source inverters," *IEEE Trans. Power Electron.*, vol. 14, no. 4, pp. 743–752, Jul. 1999.
- [12] J. Kim, J. Hong, and K. Nam, "A current distortion compensation scheme for four-switch inverters," *IEEE Trans. Power Electron.*, vol. 24, no. 3–4, pp. 1032–1040, Mar.–Apr. 2009.
- [13] S. Kouro, P. Cortés, R. Vargas, U. Ammann, and J. Rodríguez, "Model predictive control—A simple and powerful method to control power converters," *IEEE Trans. Ind. Electron.*, vol. 56, no. 6, pp. 1826–1838, 2009.
- [14] R. Wang, J. Zhao, and Y. Liu, "A comprehensive investigation of four-switch three-phase voltage source inverter based on double Fourier integral analysis," *IEEE Trans. Power Electron.*, vol. 26, no. 10, pp. 2774–2787, Oct. 2011.
- [15] C. A. Rojas, J. Rodriguez, F. Villarroel, J. R. Espinoza, C. A. Silva, and M. Trincado, "Predictive torque and flux control without weighting factors," *IEEE Trans. Ind. Electron.*, vol. 60, no. 2, pp. 681–690, Feb. 2013.
- [16] J. Rodriguez, R. M. Kennel, J. R. Espinoza, M. Trincado, C. A. Silva, and C. A. Rojas, "High-performance control strategies for electrical drives: An experimental assessment," *IEEE Trans. Ind. Electron.*, vol. 59, no. 2, pp. 812–820, Feb. 2012.
- [17] P. Cortes, J. Rodriguez, C. Silva, and A. Flores, "Delay compensation in model predictive current control of a three-phase inverter," *IEEE Trans. Ind. Electron.*, vol. 59, no. 2, pp. 1323–1325, Feb. 2012.
- [18] Y. Zhang, J. Zhu, and W. Xu, "Analysis of one step delay in direct torque control of permanent magnet synchronous motor and its remedies," in *Proc. Int. Conf. Elect. Machines S*.
- [19] M. Habibullah and D. D. C. Lu, "Predictive torque and flux control of a four-switch inverter-fed IM drive," in *Proc. 1st Int. Future Energy Electron. Conf.*, 2013, pp. 629–634.
- [20] J. Rodriguez, J. Pontt, C. A. Silva, P. Correa, P. Lezana, P. Cortes, and U. Ammann, "Predictive current control of a voltage source inverter," *IEEE Trans. Ind. Electron.*, vol. 54, no. 1, pp. 495–503, Feb. 2007.

Authors

K.Roopa Reddy

Completed B. Tech in Electrical & Electronics Engineering and MTech in Power Electronics from Aurora's Engg.colg, Bhongir, Affiliated to JNTUA. Pursuing Ph.d from JNTUH. Working as Associate Professor at ANURAG Group of Institutions (Formerly known as CVSR College of Engineering (Autonomous)) Affiliated to JNTUH, Hyderabad, Telangana, India. Area of interest includes Electrical Power System, power electronics, electrical Machines and drives control.

Akhila .V

Completed B. TECH in Electrical & Electronics Engineering in 2014 from Vignan's institute of management and technology for women affiliated to Jawaharlal University, Hyderabad and Pursuing MTech form ANURAG Group of Institutions (Formerly known as CVSR College of Engineering (Autonomous)) Affiliated to JNTUH, Hyderabad, Telangana, India. Area of interest includes Power Electronics, electrical Machines and drives control.